

Diagnostics for a 1.2 kA, 1 MeV, Electron Induction Injector

T. L. Houck,^{*} D. E. Anderson, S. Eylon, E. Henestroza, S. M. Lidia,
D. L. Vanecek, G. A. Westenskow^{*}, and S. S. Yu

^{}Lawrence Livermore National Laboratory (LLNL),
Livermore, CA 94551
Lawrence Berkeley National Laboratory (LBNL),
Berkeley, CA 94720*

Abstract. We are constructing a 1.2 kA, 1 MeV, electron induction injector as part of the RTA program, a collaborative effort between LLNL and LBNL to develop relativistic klystrons for Two-Beam Accelerator applications. The RTA injector will also be used in the development of a high-gradient, low-emittance, electron source and beam diagnostics for the second axis of the Dual Axis Radiographic Hydrodynamic Test (DARHT) Facility. The electron source will be a 3.5"-diameter, thermionic, flat-surface, m-type cathode with a maximum shroud field stress of approximately 165 kV/cm. Additional design parameters for the injector include a pulse length of over 150 ns flat top (1% energy variation), and a normalized edge emittance of less than 200π -mm-mr. Precise measurement of the beam parameters is required so that performance of the RTA injector can be confidently scaled to the 4 kA, 3 MeV, and 2-microsecond pulse parameters of the DARHT injector. Planned diagnostics include an isolated cathode with resistive divider for direct measurement of current emission, resistive wall and magnetic probe current monitors for measuring beam current and centroid position, capacitive probes for measuring A-K gap voltage, an energy spectrometer, and a pepperpot emittance diagnostic. Details of the injector, beam line, and diagnostics are presented.

INTRODUCTION

Induction accelerators are a unique source for high-current, high-brightness, electron beams. A collaboration between the Lawrence Livermore National Laboratory (LLNL) and Lawrence Berkeley National Laboratory (LBNL) has been studying the application of induction accelerators as drivers for relativistic klystrons. The relativistic klystron is a very high-power microwave source that could be used to power future linear colliders based on the Two-Beam Accelerator (RK-TBA) concept (1). As part of the collaboration, a prototype relativistic klystron is being constructed at LBNL to study issues concerning physics, engineering, efficiency, and cost (2). A major technical challenge to the successful operation of a full scale relativistic klystron is the transport of the electron beam through several hundred meters of narrow aperture microwave

extraction structures and induction accelerator cells. Demanding beam parameters are required of the electron source, an induction injector, to achieve the transport goals. The RTA injector is currently undergoing testing of its pulsed power system with beam tests scheduled in three months.

Induction accelerators are also used to produce intense x-ray sources for radiographic applications. The Dual Axis Radiographic Hydrodynamic Test (DARHT) Facility, under construction at the Los Alamos National laboratory (LANL), will use two induction accelerators. A LLNL and LBNL collaboration is designing the induction accelerator for the second axis. This accelerator, an upgrade over the first axis, will produce a 4 kA, 20 MeV, 2-microsecond electron pulse that can be “chopped” into shorter pulses to generate a series of radiographic images. The major challenge for this accelerator is achieving the required x-ray spot size. This spot size defines the maximum beam emittance at the bremsstrahlung converter. Once again, very demanding beam parameters are required at the electron source to achieve accelerator performance goals.

THE RTA INJECTOR AND DIAGNOSTIC LAYOUT

The RTA injector, depicted in Figure 1, is comprised of 24 three-core induction cells and a thermionic cathode. Beam focusing is accomplished by three large-bore solenoids installed on the central pumping spool and seven smaller solenoids located within the anode stalk. Cathode current and A-K gap voltage diagnostics are included.

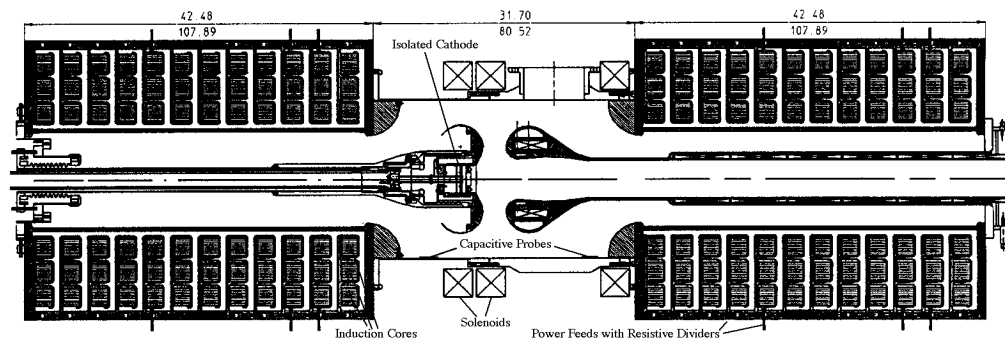


FIGURE 1. Depiction of the RTA injector indicating the locations of the isolated cathode, capacitive (dV/dt) probes, and resistive dividers for the power feeds.

The majority of the diagnostics will be installed after the injector as indicated in Figure 2. The first 1.4 m of beam line will include two beam position and current monitors to allow the offset and angle of the beam at the exit of the injector to be measured. A pop-in probe will be incorporated in a pumping port to allow the beam profile to be viewed. A pepperpot emittance diagnostic is shown in Figure 2. However, several different diagnostic packages will be installed depending on the beam parameters to be measured or diagnostics to be studied.

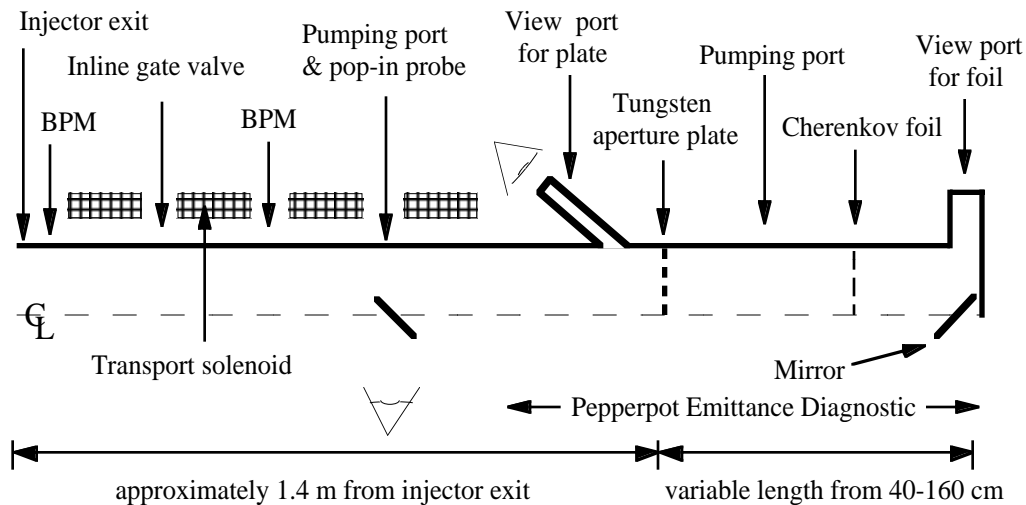


FIGURE 2. Beamline layout for emittance measurements. Other layouts will feature additional pop-in probes, an energy spectrometer, and/or an isolated beam dump.

DIAGNOSTICS

A variety of diagnostics will be used to determine the performance of the injector, both permanently installed monitors for general operational and temporary diagnostics specific to the injector commissioning and troubleshooting. A general issue for all the diagnostics is the pulse length. Recent induction accelerators at LLNL and LANL operate with pulse lengths of 50 to 80 ns. Many of the diagnostics and measurement techniques developed for those accelerators will need to be modified. For example, interceptive diagnostics such as Cherenkov foils are much more at risk of damage at the longer pulse lengths. The diagnostics to be used on the RTA injector will also serve as prototypes for the DARHT injector.

Cathode Current

An accurate measurement of the emitted current from the cathode is required both for determining the performance of the injector and benchmarking codes. Several techniques were considered and eventually rejected due to geometric, thermal, and/or reliability constraints. The final selection is to electrically isolate the cathode from the stalk and forcing the current to flow through several parallel, 0.25-inch-wide strips of 25 μm -thick nichrome foil that act as current-viewing resistors. The potential drop across the foil is measured and the current inferred. To improve the time response ($\approx L/R$), a parallel-strip shunt geometry is used where the foil is folded on itself to increase the resistance while lowering the series inductance. This well-known technique is particularly amenable for the restrictive geometry of the cathode housing.

A-K Voltage and Beam Energy

Three different methods will be used to determine the A-K voltage and beam energy. The first method involves measuring the applied voltage to the induction cores with resistive dividers at the connection of the power feeds to the induction cells. The resistive dividers are comprised of 15 similar resistors in series. This arrangement minimizes the problem of voltage dependent properties. The resistors should evenly divide the total potential drop, and the applied voltage is simply the number of resistors times the potential across any one resistor. Summing the applied voltage of all the power feeds gives the applied voltage to the A-K gap. Resistive dividers can be noisy and have a limited bandwidth. However, for our application, the bandwidth is not a limitation, as the voltage rise time is approximately 100 ns.

Capacitive dV/dt pickup probes are used for a more direct measurement of the A-K gap voltage and also to provide greater bandwidth with respect to the resistive dividers. The probe signal is approximately

$$V_s \cong (C_p Z_o) dV_o/dt, \quad (1)$$

where Z_o is the transmission line impedance and C_p is the capacitance between the electrodes and the probe. For our experiment Z_o is 50 ohms, C_p is 0.5 pF, the voltage rise time is 5×10^{12} V/s producing a signal voltage of 125 volts. The signal is then integrated to determine V_o . The minimum response time of the probe is $Z_o C_s$ where C_s is the stray capacitance between the probe and the wall. C_s is approximately 100 pF producing a response time of 5 ns. The maximum time is set by the integrator. We use printed circuits for our capacitive probes as illustrated in Figure 3. At least two probes, separated longitudinally, are required to resolve the contributions from the anode and cathode halves of the injector.

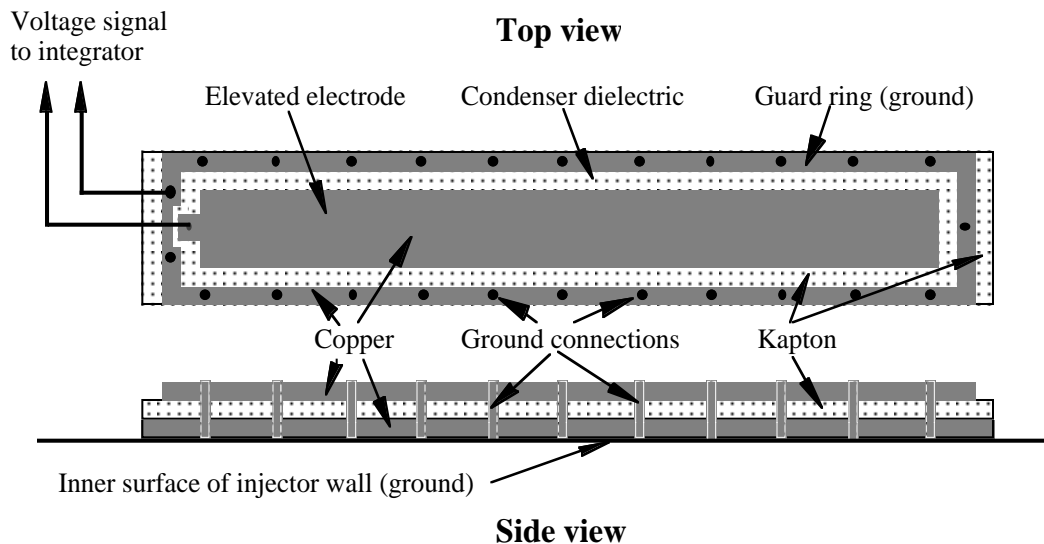


FIGURE 3. Schematic of the printed circuit capacitive dV/dt pickup probe.

A conventional energy spectrometer comprised of an on-axis collimator, dipole magnet, scintillator, and viewing port will be used to directly measure beam. By varying the beam radius at the entrance of the graphite collimator, the current density at the scintillator can be adjusted. The spectrometer is on loan from LANL where it was calibrated to 1% accuracy in absolute energy. Relative variations in beam energy can be determined to 0.1% and the total energy variation that can be imaged across the scintillator is about 5%. A streak camera will be used to look at energy variations across the flat-top portion of the pulse. A gated camera will be used to examine the beam energy during specific time slices of the pulse, e.g. during the rise time.

Beam Current and Centroid Position

Two different methods will be used to determine the beam current and centroid position. Magnetic pickup (B-dot) loops will determine the time derivative of the current pulse. The voltage induced on the loop can then be integrated to recover the current. Our B-dot loop diagnostics will consist of eight loops evenly spaced around the inner diameter of a one-inch-thick flange. The loops are recessed into the flange to avoid beam interception. Four evenly spaced loops are summed to minimize the error in total current due to offsets in beam centroid. Geometrically opposite pairs are differenced to generate signals that are proportional to the centroid offset. The B-dot loops have the advantage of simple construction and a broad frequency response. The principle disadvantage is the requirement for integrators.

Resistive wall current monitors measure the potential drop of the return wall current across a known resistance generating a signal proportional to the current. Our monitors will consist of 25 μm -thick nichrome foil that spans a short insulated break around the circumference of the beam tube wall and have a total resistance of a few milliohms. The diameter of the foil matches the inner diameter of the beam tube to avoid discontinuity in the beam pipe wall. An inductive material is placed outside of the foil to force the wall current to flow through the foil. The time response of the monitor, determined by the series inductance and resistance, is about 5 ns. The parallel inductance of the monitor will cause the signal to decay or "droop." This is expected to be small, but noticeable, for the 250 ns FWHM pulse length. The output signal can be corrected for known droop in the diagnostic through compensation circuits, either passive or active. Alternatively, for digitized signal data, the correction can be done with analysis software. Eight voltage pickoffs evenly spaced around the diameter of the foil are used to determine beam current and centroid position, similar to the B-dot loops. The sensitivity of the monitor is approximately a volt per kiloampere of current. The resistive wall current monitors have the advantage of producing a signal proportional to the current. However, the frequency response is less than that of B-dot loops.

The beam dump will be electrically isolated through nichrome film (current-viewing resistors) similar to the cathode to allow for the measurement of the total current deposited in the dump. However, the centroid position will not be determined.

The errors inherent in the above monitors for off-axis beams are easily calculated and not expected to be an issue. The major concern is in the calibration of the diagnostics. The nominal tolerance for commercial components used in the monitors would limit accuracy to about 5%. By calibrating complete systems, i.e. the individual diagnostic with cables, integrators, and compensation circuits, as applicable, we hope to achieve accuracies approaching 1%.

Current Density Profile

The current density profile will be measured using Cherenkov and/or optical transition radiation from intercepting foils. A primary concern with using foils is possible damage from beam energy deposition. Average heating of the foil can be controlled by adjusting the repetition rate of the injector. The difficulty lies in the single-shot heating where material can be melted and ejected before the heat is conducted away. If the foils are sufficiently thin that the radiation generated by bremsstrahlung escapes, assuming the beam pulses are short compared to the thermal conduction time, the temperature rise in the foil is approximately:

$$\Delta T = \frac{J\Delta t}{\rho C_p e} \left[\frac{dT_e}{dz} \right]_c, \quad (2)$$

where J is the current density, Δt is the pulse length, ρ and C_p are the density and specific heat of the foil, respectively, and $[dT_e/dz]_c$ is the collisional stopping power for the electrons. For a given foil material, the minimum beam radius at intercept can be determined from Equation 2. Since the collisional stopping power is reasonably constant with energy for relativistic electrons, Equation 2 may also be used to scale the measured performance of the foils to the higher energy of the DARHT injector. For example, the minimum beam diameter to avoid damage for a 1 kA, 300 ns, relativistic electron beam pulse on a thin quartz foil is about 2 cm. We anticipate using a number of foil materials, including kapton, quartz, graphite, tantalum, and tungsten.

The light generated at the beam/foil interaction will be recorded using both gated and streak cameras. The streak camera will be used principally to determine if the properties of the foil and/or beam change during the pulse. The significant levels of energy deposited in the foil could affect the dielectric constant or generate a surface plasma that could be confused as a variation in beam parameters.

Emittance

Measuring the beam emittance is expected to be very difficult as the beam is highly space charge dominated. A pepperpot emittance diagnostic is being constructed. The effect of space charge can be appreciated by considering the envelope equation for a round, uniform beam in a drift region:

$$\frac{d^2 R}{dz^2} = \frac{\epsilon^2}{R^3} + \frac{2I}{RI_A(\beta\gamma)^3}, \quad (3)$$

where R is beam radius (edge), ϵ is the unnormalized edge emittance, and $I_A = 17$ kA. The cathode is in a magnetic field free region. We desire for the emittance to dominate space charge effects for the beamlets in the region following the pepperpot, i.e.

$$\frac{\epsilon_n^2}{R_b^2} \gg \frac{2I}{\beta\gamma_A}, \quad \text{or} \quad \epsilon_n^2 \gg \frac{I_b h^2}{2\beta\gamma_A}, \quad \text{where} \quad I = \left(\frac{h}{2R_b} \right)^2 I_b. \quad (4)$$

R_b and I_b are the beam radius and current at the front of the pepperpot, and h is the aperture. The size of the aperture is the only variable for adjusting the relative contribution of emittance to space charge. For the designed RTA injector beam parameters, 1.2 kA, 1 MeV and 100 π -mm-mr, and using a 250 μm aperture, the emittance term is approximately an order of magnitude larger than the space charge. Our aperture plate will consist of a rectangular pattern of 121 (11 \times 11) 250 μm apertures with 7 mm spacing on a 500 μm thick tungsten plate. The tungsten plate represents about two range thickness for 1 MeV electrons. A second 1 mm-thick tungsten plate with nominal 750 μm apertures will be placed in front of the thinner plate to improve thermal conduction. At four locations, apertures will not be drilled in the thicker plate to assist in determining background and orientation. The beamlets will strike a quartz foil located 80 cm (adjustable from 40 to 160 cm) after the aperture plate. The Cherenkov light generated at the foil will be imaged with a gated camera.

Small effects such as the aperture plate thickness (vignetting), fringe fields from the upstream solenoids, and beam waist location will be accounted for in the data analysis. A more serious problem concerns the effect of the conductive aperture plate on the beam. It has been demonstrated (3) that, while the local distribution in phase space can be determined, the global $x-x'$ curve is dominated by the non-linear focusing of the aperture plate. E-Gun simulations performed for our beam parameters indicate that the beam emittance determined from the pepperpot data will be as much as six times the actual emittance in the absence of the aperture plate. This effect can be accounted for in the analysis. However, the accuracy in the final emittance value will suffer. Note that this is only an issue for space charge dominated beams where aperturing is required.

An alternative to the pepperpot diagnostic is to vary the focusing of the beam and look at changes in the radial profile of the beam. The most straight forward method will be to insert a nonconducting foil a short distance after a solenoid. The strength of the solenoid could then be increased causing the focus to move through the foil. Matching the observed radius variation with the applied solenoidal field to computer simulations will allow the emittance to be inferred. Once again, the issue will be the minimum beam spot size that the foil can tolerate. By operating in an over-focus regime, i.e. the beam waist always remains in front of the foil, it may be possible to limit the minimum beam radius at the foil, but still generate significant variations in radius. We are also studying the effect of using a quadrupole magnet to focus in a single plane. This will reduce the issue of current density, but limit the emittance measurement to a single plane.

SUMMARY

A variety of diagnostics will be used to characterize the beam produced by the RTA injector. These diagnostics have been extensively developed over the past decade for use on induction injectors/accelerators. However, the challenge for the RTA program is to adapt these diagnostics for pulse lengths a factor of four longer, and, in the development of diagnostics for the DARHT second axis, a factor of nearly 40 longer. Determining emittance of the highly space charge dominated beam will also require new levels of precision and/or technique.

ACKNOWLEDGMENTS

Many people have provided advice and insight regarding our diagnostic issues. In particular, we thank Tom Fesseden, Bill Fawley, and Mike Vella of LBL, and Dave

Moir and Mike Brubecker of LANL. The work was performed under the auspices of the U.S. Department of Energy by LLNL under contract W-7405-ENG-48, and by LBNL under contract AC03-76SF00098.

REFERENCES

- [1] Sessler, A. M., S. S. Yu, *Phys. Rev. Lett.*, **54**, 889 (1987).
- [2] Houck, T. L., et al., *IEEE Trans. Plasma Sci.*, **24**, 938–946 (1996).
- [3] Hughes, T. P., R. L. Carlson, D. C. Moir, *J. Appl. Phys.*, **68**, 2562–2571 (1990).